Classifying DME vs Normal SD-OCT volumes: A replicable comparison

Joan Massich, Désiré Sidibé
LE2I UMR6306, CNRS, Arts et Métiers
Univ. Bourgogne Franche-Comté
12 rue de la Fonderie
71200 Le Creusot, France

Email: joan.massich@u-bourgogne.fr

Mojdeh Rastgoo, Guillaume Lemaître
ViCOROB, Universitat de Girona
Campus Montilivi, Edifici P4
17071 Girona, Spain

Carol Y. Cheung, Tien Y. Wong, Ecosse Lamoureux, Dan Milea
Singapore Eye Research Institute
Singapore National Eye Center, Singapore

Fabrice Mériaudeau
UTP

Abstract—
Index Terms—

I. INTRODUCTION

Eye diseases such as Diabetic Retinopathy (DR) and Diabetic Macular Edema (DME) are the most common causes of irreversible vision loss in individuals with diabetes. Just in United States alone, health care and associated costs related to eye diseases are estimated at almost $500\,M$ [1]. Moreover, the prevalent cases of DR are expected to grow exponentially affecting over $300\,M$ people worldwide by 2025 [2]. Given this scenario, early detection and treatment of DR and DME play a major role to prevent adverse effects such as blindness. DME is characterized as an increase in retinal thickness within 1 disk diameter of the fovea center with or without hard exudates and sometimes associated with cysts [3]. Fundus images which have proven to be very useful in revealing most of the eye pathologies [4, 5] are not as good as Optical Coherence Tomography (OCT) images which provide information about cross-sectional retinal morphology [6]. old

Many of the previous works on OCT image analysis have focused on the problem of retinal layers segmentation, which is a necessary step for retinal thickness measurements [7, 8]. However, few have addressed the specific problem of DME and its associated features detection from OCT images. Figure 1 shows one normal B-scan and two abnormal B-scans. old

Evaluation of the volumetric scan is time consuming, expensive and some pathology signs are easy to miss [9]

~~· coexistence of multiple pathologies [10] · OCT image acquisition has drift [10] · variability in shape, size and magnitude within the same pathology [10] · retina reflectivity (schuman 2014) [10] · inconsistent image quality (barnum 2008) [10]~~ sik

~~This article is structured as follows: Background(Sect. ??) offers a general idea of the methods reviwed. Materials and~~
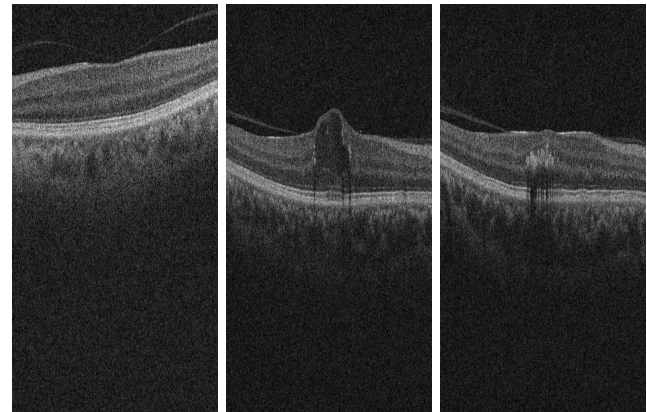
(a) Normal (b) DME-cyst (c) DME-exudate

Fig. 1. Example of SD-OCT images for normal (a) and DME patients (b)-(c) with cyst and exudate, respectively.

~~methods discusses data and mapping of the methodologies to our framework. Results offers (Sect. V) (a) individual results of each methodology, as well as our strategy followed to validate that our implementation complies with the results reported by the original work (b) comparative results of the best methodlogy configurations to drive our discussion. Discussion(Sect. VI). Conclusion and Further work(Sect. VII).~~ sik

II. BACKGROUND

This section reviews works straightly addressing the problem of classifying OCT volumes as normal or abnormal, regardless of the target pathology. The methods are categorized in terms of its learning strategy, namely: supervised or semi-supervised.

This section reviews the works straightly addressing the problem of classifying OCT volumes as normal or abnormal. old

Implementation details in order to integrate all these methodologies in a common framework can be found in Sect. IV and further details in all the repositories available [?, ?, ?, ?, ?].

A. Srinivasan

Srinivasan *et al.* [11] proposed a classification method to distinguish DME, Age-related Macular Degeneration (AMD) and normal SD-OCT volumes. The OCT images are preprocessed by reducing the speckle noise by enhancing the sparsity in a transform-domain and flattening the retinal curvature to reduce the inter-patient variations. Then, Histogram of Oriented Gradients (HOG) are extracted for each slice of a volume and a linear Support Vector Machines (SVM) is used for classification. On a dataset of 45 patients equally subdivided into the three aforementioned classes, this method leads to a correct classification rate of 100%, 100% and 86.67% for normal, DME and AMD patients, respectively. The images that have been used in their paper, are publicly available but are already preprocessed (i.e., denoised), have different sizes for the OCT volumes, do not offer a huge variability in term of DME lesions, and some of them, without specifying which, have been excluded for the training phase; all these reasons prevent us from using this dataset to benchmark our work. old

B. Venhuizen

Venhuizen *et al.* proposed a method for OCT images classification using the Bag-of-Words (BoW) models [9]. The method starts with the detection and selection of keypoints in each individual B-scan, by keeping the most salient points corresponding to the top 3% of the vertical gradient values. Then, a texton of size 9×9 pixels is extracted around each keypoint, and Principal Component Analysis (PCA) is applied to reduce the dimension of every texton to get a feature vector of size 9. All extracted feature vectors are used to create a codebook using k-means clustering. Then, each OCT volume is represented in terms of this codebook and is characterized as a histogram that captures the codebook occurrences. These histograms are used as feature vector to train a Random Forest (RF) with a maximum of 100 trees. The method was used to classify OCT volumes between AMD and normal cases and achieved an Area Under the Curve (AUC) of 0.984 with a dataset of 384 OCT volumes. old

C. Liu

Liu *et al.* proposed a methodology for detecting macular pathology in OCT images using Local Binary Patterns (LBP) and gradient information as attributes [10]. The method starts by aligning and flattening the images and creating a 3-level multi-scale spatial pyramid. The edge and LBP histograms are then extracted from each block of every level of the pyramid. All the obtained histograms are concatenated into a global descriptor whose dimensions are reduced using PCA. Finally a SVM with an Radial Basis Function (RBF) kernel is used as classifier. The method achieved good results in detection OCT scan containing different pathology such as DME or AMD, with an AUC of 0.93 using a dataset of 326 OCT scans. old

Type of Lesions	#		Type of Lesions	#	
Vitreomacular Traction	4		Fluid with HE and cystoid spaces	1	
Cystoid spaces with Hard Exudates (HE) causing central retinal thickening	1		Cystoid spaces causing parafoveal retinal thickening	1	
Cystoid spaces causing central and parafoveal retinal thickening	1		CSR with HE causing retinal thickening	2	
Retinal thickening	2		Cystoid spaces causing retinal thickening	3	
CSR(subretinal fluid) causing central and parafoveal thickening	1				

Figure 2. Example of the DME dataset

Fig. 2. Experimental Setup

D. Desire

E. Khaled Alsaih

F. Lemaitre

The proposed method by Lemaitre *et al.* [12] is based on LBP features to describe the texture of OCT images and dictionary learning using the BoW models [13]. Our later study proposes a standard classification procedure to differentiate between DME and normal SD-OCT volumes [14]The data is pre-processed using Non-Local Means (NLM) filtering. The volumes are mapped into discrete set of structures namely: local, when these structures correspond to patches; or global, when the structures correspond to volume slices or the whole volume. These structures are described in terms of texture using LBP or LBP from Three Orthogonal Planes (LBP-TOP) and encoded using histogram, PCA or BoW to produce a single feature vector in order to present the volumes to a RF classifeir. This methodology was tested against Venhuizen *et al.* [9] using public and non-public datasets showing an improvement within the results achieving a Sensitivity (SE) of 87.5% and a Specificity (SP) of 75%. old

III. DATA

~~Despite Venhuizen et al. tested on a public dataset [?], this dataset is intended to AMD. Srinivasan also tested on a public dataset [?], however the images are cropped and filtered etc. So thats why we collected the SERI dataset.~~ sik

This dataset was acquired by the Singapore Eye Research Institute (SERI), using CIRRUS TM (Carl Zeiss Meditec, Inc., Dublin, CA) SD-OCT device. The dataset consists of 32 OCT volumes (16 DME and 16 normal cases). Each volume contains 128 B-scan with resolution of 512×1024 pixels. All SD-OCT images are read and assessed by trained graders and identified as normal or DME cases based on evaluation of retinal thickening, hard exudates, intraretinal cystoid space formation and subretinal fluid. old

IV. EXPERIMENTAL SETUPMATERIALS AND METHODS[sik]

The experimental set-up is formulated as a standard classification procedure consisting of 5 steps. Figure 3 outlines these 5 steps and illustrates how the methodologies have been translated to such schema.

A. method comments[sik]

> here goes a description left to right of the modules, making remarks of the difference between the needs of each method.

First, the OCT volumes are pre-processed as presented in details in Sect. **??**. Then, LBP and LBP-TOP features are detected, mapped and represented as discussed in depth in Sect. **??**, Sect. **??**, and Sect. **??**, respectively. Finally, the classification step is presented in Sect. **??**. old

The mapping in A is computed in this manner while in B this comes on the other side bla bla bla[sik]

B. Validation

All the experiments are evaluated in terms of SE and SP using the Leave-One-Patient Out Cross-Validation (LOPO-CV) strategy, in line with [12]. SE and SP are statistics driven from the confusion matrix (see Fig. **??**) as stated in Eq. (1). The SE evaluates the performance of the classifier with respect to the positive class, while the SP evaluates its performance with respect to negative class. old

$$ SE = \frac{TP}{TP + FN} \qquad SP = \frac{TN}{TN + FP} \tag{1} $$

The use of LOPO-CV implies that at each round, a pair DME-normal volume is selected for testing while the remaining volumes are used for training. Subsequently, no SE or SP variance can be reported. However, LOPO-CV strategy has been adopted despite this limitation due to the reduced size of the dataset. old

C. Management of data depending terms

Be aware that when computing the GMM [?], or the dictionary [?], only the training data for the current fold is used. Therefore such modules are recomputed at each fold. [sik] Other parameter tuning such the case of XXXX and YYYYY are also carried out using only ZZZZ [sik]

V. RESULTS

VI. DISCUSSION

VII. CONCLUSION AND FURTHER WORK

REFERENCES

[1] S. Sharma, A. Oliver-Hernandez, W. Liu, and J. Walt, "The impact of diabetic retinopathy on health-related quality of life," *Current Opinion in Ophtalmology*, vol. 16, pp. 155–159, 2005.

[2] S. Wild, G. Roglic, A. Green, R. Sicree, and H. King, "Global prevalence of diabetes estimates for the year 2000 and projections for 2030," *Diabetes Care*, vol. 27, no. 5, pp. 1047–1053, 2004.

[3] Early Treatment Diabetic Retinopathy Study Group, "Photocoagulation for diabetic macular edema: early treatment diabetic retinopathy study report no 1," *JAMA Ophthalmology*, vol. 103, no. 12, pp. 1796–1806, 1985.

[4] M. R. K. Mookiah, U. R. Acharya, C. K. Chua, C. M. Lim, E. Ng, and A. Laude, "Computer-aided diagnosis of diabetic retinopathy: A review," *Computers in Biology and Medicine*, vol. 43, no. 12, pp. 2136–2155, 2013.

[5] E. Trucco, A. Ruggeri, T. Karnowski, L. Giancardo, E. Chaum, J. Hubschman, B. al Diri, C. Cheung, D. Wong, M. Abramoff, G. Lim, D. Kumar, P. Burlina, N. M. Bressler, H. F. Jelinek, F. Meriaudeau, G. Quellec, T. MacGillivray, and B. Dhillon, "Validation retinal fundus image analysis algorithms: issues and proposal," *Investigative Ophthalmology & Visual Science*, vol. 54, no. 5, pp. 3546–3569, 2013.

[6] Y. T. Wang, M. Tadarati, Y. Wolfson, S. B. Bressler, and N. M. Bressler, "Comparison of Prevalence of Diabetic Macular Edema Based on Monocular Fundus Photography vs Optical Coherence Tomography," *JAMA Ophthalmology*, pp. 1–7, Dec 2015.

[7] S. J. Chiu, X. T. Li, P. Nicholas, C. A. Toth, J. A. Izatt, and S. Farsiu, "Automatic segmentation of seven retinal layers in sd-oct images congruent with expert manual segmentation," *Optic Express*, vol. 18, no. 18, pp. 19 413–19 428, 2010.

[8] R. Kafieh, H. Rabbani, M. D. Abramoff, and M. Sonka, "Intra-retinal layer segmentation of 3d optical coherence tomography using coarse grained diffusion map," *Medical Image Analysis*, vol. 17, pp. 907–928, 2013.

[9] F. G. Venhuizen, B. van Ginneken, B. Bloemen, M. J. P. P. van Grisven, R. Philipsen, C. Hoyng, T. Theelen, and C. I. Sanchez, "Automated age-related macular degeneration classification in OCT using unsupervised feature learning," in *SPIE Medical Imaging*, vol. 9414, 2015, p. 94141l.

[10] Y.-Y. Liu, M. Chen, H. Ishikawa, G. Wollstein, J. S. Schuman, and R. J. M., "Automated macular pathology diagnosis in retinal oct images using multi-scale spatial pyramid and local binary patterns in texture and shape encoding," *Medical Image Analysis*, vol. 15, pp. 748–759, 2011.

[11] P. P. Srinivasan, L. A. Kim, P. S. Mettu, S. W. Cousins, G. M. Comer, J. A. Izatt, and S. Farsiu, "Fully automated detection of diabetic macular edema and dry age-related macular degeneration from optical coherence tomography images," *Biomedical Optical Express*, vol. 5, no. 10, pp. 3568–3577, 2014.

[12] G. Lemaitre, M. Rastgoo, J. Massich, S. Sankar, F. Meriaudeau, and D. Sidibe, "Classification of SD-OCT volumes with LBP: Application to dme detection," in *Medical Image Computing and Computer-Assisted Intervention (MICCAI), Ophthalmic Medical Image Analysis Workshop (OMIA)*, 2015.

[13] J. Sivic and A. Zisserman, "Video google: a text retrieva approach to object matching in videos," in *IEEE ICCV*, 2003, pp. 1470–1477.

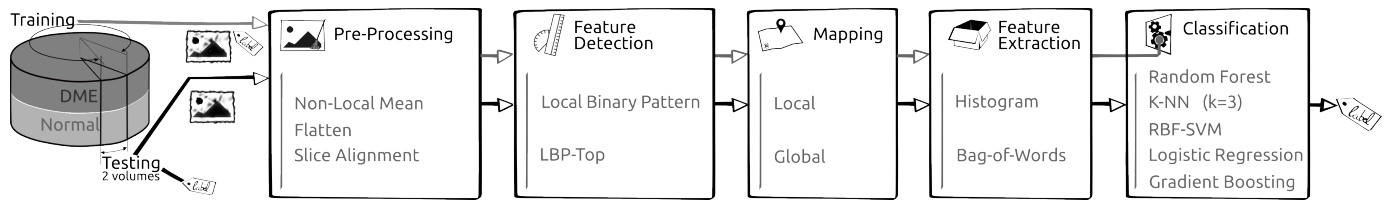[14] G. Lemaitre, M. Rastgoo, and J. Massich, "retinopathy: Jo-omia-2015," Nov. 2015. [Online]. Available: http://dx.doi.org/10.5281/zenodo.34277

Fig. 3. Experimental Setup

TABLE I
SUMMARY OF THE STATE-OF-THE-ART METHODS.

Ref	Diseases			Data size	Pre-processing				Features	Representation	Classifier	Evaluation	Results
	AMD	DME	Normal		De-noise	Flatten	Aligning	Cropping					
[11]	✓	✓	✓	45	✓	✓		✓	HOG		linear-SVM	Accuracy (ACC)	86.7%,100%,100%
[9]	✓		✓	384					Texton	BoW, PCA	RF	AUC	0.984
[10]	✓	✓	✓	326		✓	✓		Edge, LBP	PCA	SVM-RBF	AUC	0.93
[12]		✓	✓	62	✓				LBP-LBP-TOP	PCA, BoW, histogram	RF	SE,SP	87.5%, 75%